Astron. Astrophys. 141, 309–317 (1984)

ASTRONOMY AND ASTROPHYSICS

The distribution of neutral hydrogen in the Sombrero galaxy, NGC 4594

E. Bajaja[1,2,*], G. van der Burg[3], S. M. Faber[4], J. S. Gallagher[5,], G. R. Knapp[6], and W. W. Shane[3,2]**

[1] Instituto Argentino de Radioastronomia, Casilla de Correo No. 5, (1894) Villa Elisa (Prov. de Bs. As.), Argentina
[2] Sterrewacht te Leiden, Postbus 9513, 2300 RA Leiden, The Netherlands
[3] Sterrenkundig Instituut, Katholieke Universiteit, Toernooiveld, 6525 ED Nijmegen, The Netherlands
[4] Lick Observatory, Board of Studies in Astronomy and Astrophysics, University of California, Santa Cruz, CA 95064, USA
[5] Dept. of Astronomy, University of Illinois, 1011 W. Springfield Ave., Urbana, IL 61081, USA
[6] Dept. of Astrophysical Sciences, Princeton University, Princeton, USA

Received April 18, accepted July 9, 1984

Summary. Fan beam observations with an E-W resolution of 11′.4 of NGC 4594 (the Sombrero galaxy) in the 21-cm line, made with the Westerbork Synthesis Radio Telescope, are reported. The results are presented in the form of a position-velocity contour map. The global properties of the galaxy are: $M_{HI}=1.3\ 10^9\ M_\odot$ (distance 18.6 Mpc), $[M_{HI}/L_B]=0.010$ and $V_{sys}=1100\ km\ s^{-1}$ (heliocentric). A model is proposed which reproduces the gross properties of the H I distribution. The gas appears to be confined to an annulus between radii 12 and 19 kpc, coincident with the distribution of dust in the galaxy, and to be concentrated within this annulus into two concentric rings. The rotation velocity in this region is about 370 km s^{-1} and is either constant or slightly decreasing with radius. The velocity distribution in the annulus shows that radial motions are less than about 15 km s^{-1}, arguing against recent explosive or accretion phenomena.

The relative H I content $[M_{HI}/L_B]$ is very much lower for this galaxy than for other Sa galaxies and is lower than for H I-rich ellipticals. The H I distribution suggests that only gas outside the optical bulge has been able to survive. Mechanisms causing the removal of gas from the spheroid of the galaxy are briefly discussed.

Key words: NGC 4594 - early-type galaxies - 21-cm line

1. Introduction

In this paper, we present aperture synthesis observations of the H I distribution in NGC 4594 (M 104), the "Sombrero" galaxy, classified Sa to Sb. The galaxy has a well-developed stellar disk with an approximately exponential brightness distribution (van Houten, 1961); however the optical structure of the bulge resembles that of a giant elliptical galaxy (cf. Faber et al., 1977, hereafter FBGK). The bulge is very large, with a diameter of 285 kpc at the assumed distance of 18.6 Mpc (Burkhead, 1979); its surface brightness distribution follows a de Vaucouleurs law, and its velocity dispersion is large ($\sigma_* = 210$ km s^{-1}: Williams, 1977; Kormendy and Illingworth, 1982). The galaxy also contains a compact nuclear radio continuum source with an inverted spectrum (de Bruyn, 1978; Shaffer and Marsher, 1979). While H I emission has been detected from the galaxy (FBGK), the relative H I content $[M_{HI}/L_B]$ is much lower than the values typical for early-type spirals (e.g. Bottinelli et al., 1980), is lower than values for gas-rich ellipticals, and is lower than the sensitive upper limits set for many normal ellipticals. The galaxy is isolated, with no known companions, and the photometry of van Houten (1961) suggests that the disk has the peculiar property that the radial distributions of the light and of the dust are quite different, with the dust lying in an annulus outside the bright part of the stellar disk.

Observations of the distribution of the interstellar H I in this galaxy are therefore of interest for at least two reasons. As discussed by FBGK, the motions of the gas disk provide a probe of the mass distribution of an elliptical-like system that is relatively free of the model-dependent uncertainties which are present in mass estimates from stellar velocity dispersions. In addition, the properties of the gas disk might be useful for understanding the state of the interstellar matter in early-type galaxies.

Despite its southerly declination (−11°), NGC 4594 is a good candidate for observation with the Westerbork Synthesis Radio Telescope (WSRT) because of its east-west orientation and edge-on aspect. At this declination the telescope is a fan-beam instrument with resolution only in the east-west direction.

The first WSRT observations of NGC 4594 were made in 1972 using the provisional line receiver. A marginal detection was achieved (Bajaja and Shane, 1981) which, despite the very weak signal, pointed toward some of the results discussed here.

In Sect. 2 we describe the observations and the reduction procedure and in Sects. 3 and 4 the results and their interpretation. In Sect. 5 we discuss the global properties of the galaxy and of its interstellar medium, and in Sect. 6 we present some conclusions.

Send offprint requests to: W.W. Shane
* Member of the Carrera del Investigador Científico del Consejo Nacional de Investigaciones Científicas y Técnicas.
** Present address: Kitt Peak National Observatory, P.O. Box 26732, Tucson, AZ 85726, USA

2. Observations and reductions

NGC 4594 was observed with the WSRT during two nine-hour periods in 1981, on 27 and 28 February and 19 and 20 March (UT). The baselines ranged from 54 m to 2754 m in steps of 36 m;

the synthesized beam has half power dimensions of 11″.4 × 81″.6 ($\alpha \times \delta$). The system temperature was 55 K. The digital line backend (Bos et al., 1981) was used to observe a single polarization in 63 channels over a total bandwidth of 5 MHz; the resulting channel separation is 16.6 km s^{-1}. The data were Hanning smoothed to give a half-power channel width of 33 km s^{-1}. (Velocities in this paper are heliocentric and are calculated according to the conventional optical definition.) Both observations appeared to be of good quality and it was not necessary to delete any data. The two observations were combined and reduced as a single unit.

The continuum data were Fourier-transformed to a map and examined for the presence of continuum sources in the field. A list of the detected sources and their 1.4 GHz fluxes is given in Table 1. The positions and fluxes of the point sources were determined by fitting the antenna pattern to the data. Extended sources, however, were resolved into components with the aid of a "clean" algorithm (sometimes after subtraction of an initial point source) and the fluxes and positions are the sums and flux-weighted averages of these components. Among the continuum sources in Table 1 is the nuclear point source of NGC 4594; the flux of this source for the epoch of observation is 72.1 ± 1.1 mJy, showing no significant change from published values.

The strongest point sources in the field were subtracted from the data which were then Fourier-transformed to produce a sky map at each velocity. For two extended sources, some residual grating rings appeared close to the position of NGC 4594. These residual grating rings were removed from all channel maps using the resolution into components on the continuum map and the "clean" procedure described by Högbom (1974).

Because the galaxy is essentially edge-on and east-west (i = 85°, van Houten, 1961) and the instrumental resolution perpendicular to the equator is 82″, there is no information in the observations about the distribution of gas perpendicular to the major axis of the image. We therefore constructed a one-dimensional map of the H I distribution by taking a cross-cut along the major axis (p.a. = 90°). This map, a position-velocity (or l-v) map, consisted of 60 rows each of 512 points, spaced at intervals of 4″.5. Three channels, one at the lowest velocity and two at the highest velocities, were deleted because of band-edge effects. All further data reduction was done in this l-v plane.

The initial continuum correction map was made by averaging at each right ascension point over all velocities outside a widely chosen mask whose velocity limits varied with right ascension, leaving only grid points without line emission. This continuum map was then subtracted from the l-v map.

Due to the finite (though small) width of the galaxy in declination compared with the synthesized antenna pattern in this direction, a slight attenuation is introduced by using only one declination from each channel map. This has been evaluated by comparing this map with a map made by averaging three successive rows in declination, properly normalized by the antenna pattern. We found a small systematic residual, close to the noise level, suggesting an attenuation of about 5%, independent of position and velocity. We have continued to use the original single-declination strip scan because of its slightly better signal-to-noise ratio, but all fluxes have been corrected for this small effect.

The negative declination of NGC 4594 makes it impossible to achieve complete spatial coverage with the interferometers of the WSRT. The available coverage produces a synthesized antenna pattern with pronounced negative side-lobes in the E-W direction, as illustrated in Fig. 1 (curve a), where the maximum negative amplitude is 31% of the central peak. The effect of these side-lobes overlapping the central peak is to make extended features, even well above the theoretical detection level, unidentifiable on the original maps. This applies not only to visual inspection but also to the cleaning algorithm, which fails to find these peaks amongst the noise. Clearly these side-lobes must be removed by cleaning, but first the peaks must be made visible

Table 1. Radio continuum sources in the field

α_{1950}	δ_{1950}	S_{1415} mJy	Notes
$12^h35^m31^s.46 \pm 0^s.07$	−11°42′53″.4 ± 4″.7	90.8 ± 11.5	
12 35 48.59	−11 20 2.3	102.9 ± 2.6	E
12 36 8.82 ± 0.04	−11 20 2.1 ± 1.2	76.8 ± 3.3	
12 36 46.06 ± 0.05	−11 12 38.7 ± 1.9	18.1 ± 0.7	
12 37 22.27 ± 0.06	−11 42 22.9 ± 3.4	24.5 ± 2.3	N
12 37 23.39 ± 0.04	−11 20 54.7 ± 1.1	72.1 ± 1.1	C
12 37 36.03 ± 0.05	−11 47 36.7 ± 2.1	86.8 ± 8.5	
12 37 47.76 ± 0.06	−11 31 41.4 ± 3.8	10.4 ± 0.9	N, D
12 37 50.19 ± 0.05	−11 31 29.4 ± 2.7	15.6 ± 1.0	N, D
12 37 55.76	−11 10 16.0	70.4 ± 2.7	E
12 38 1.32 ± 0.04	−11 4 57.8 ± 1.1	115.3 ± 4.9	
12 38 29.40	−11 39 47.7	183.4 ± 10.5	E
12 38 34.98 ± 0.06	−11 27 56.3 ± 3.1	20.8 ± 1.7	
12 39 23.92 ± 0.07	−11 23 23.7 ± 4.2	51.5 ± 6.5	N

Notes: C = central continuum source of NGC 4594; D = both sources marked with a D comprise possibly one double source; E = extended source; N = not subtracted from the data

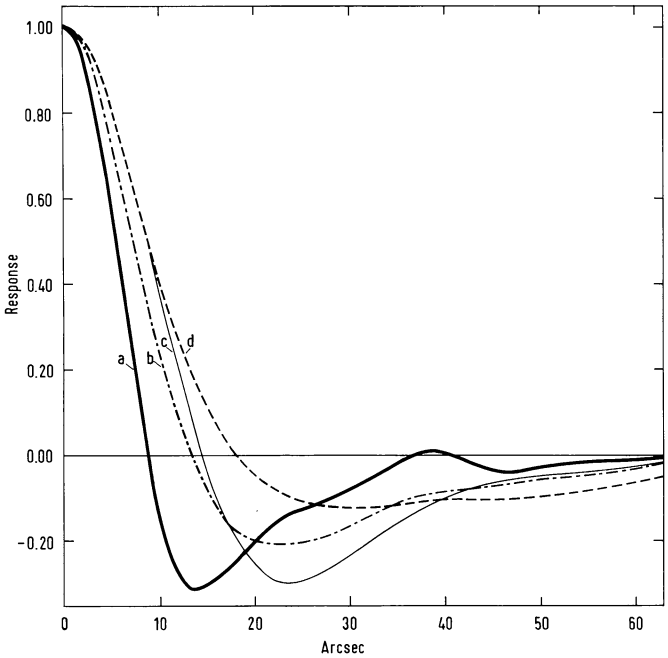

Fig. 1. Curve a: east-west crosscut of the synthesized antenna pattern expressed as a function of the distance, x, from the central peak, in grid points; Curves b and d: antenna pattern convolved with an exponential function, $\exp(-|x|/2)$ and $\exp(-|x|/4)$ respectively; Curve c: antenna pattern convolved with a Gauss function, $\exp(-x^2/8)$

by suppressing the side-lobes. Convolution with the gaussian function (Fig. 1, curve c) does not suffice, but an exponential function (Fig. 1, curves b and d) substantially reduces the amplitude of the side-lobes while only slightly broadening the central peak.

In order to retain the maximum resolution, the cleaning was done in an iterative way. The original map was cleaned to a conservative level (about 2.5 σ), the components which were found were subtracted and the resultant map and the antenna pattern convolved as shown in Fig. 1, curve b. This map was then cleaned and the components found in this step were also subtracted from the resultant map described above, giving a full-resolution map from which both sets of components had been subtracted. A broader convolution was applied and the process repeated. The fourth (and last) cleaning step, now carried to a level of 1 σ, was applied to the map as convolved to the antenna pattern shown in Fig. 1, curve d. Finally all of the delta-function components found in the above iterations were subtracted from the original map and restored (i.e. added to the residual map using only the central maximum of the unconvolved antenna pattern).

In the original continuum subtraction, the far side-lobes of the line radiation were subtracted along with the continuum. In order to compensate for this, an additional continuum correction map was made in the same way as the first correction map, but using a mask with smaller dimensions and applying it to the cleaned map. This second correction map was subtracted from the same cleaned l-v map, and the result, after primary beam correction, is shown in Fig. 2a. This map is used in the subsequent analysis. The r.m.s. noise is about 0.07 mJy arcsec^{-1}; the lowest positive contour is 0.10 mJy arcsec^{-1}, and the other contours are integral multiples of this number.

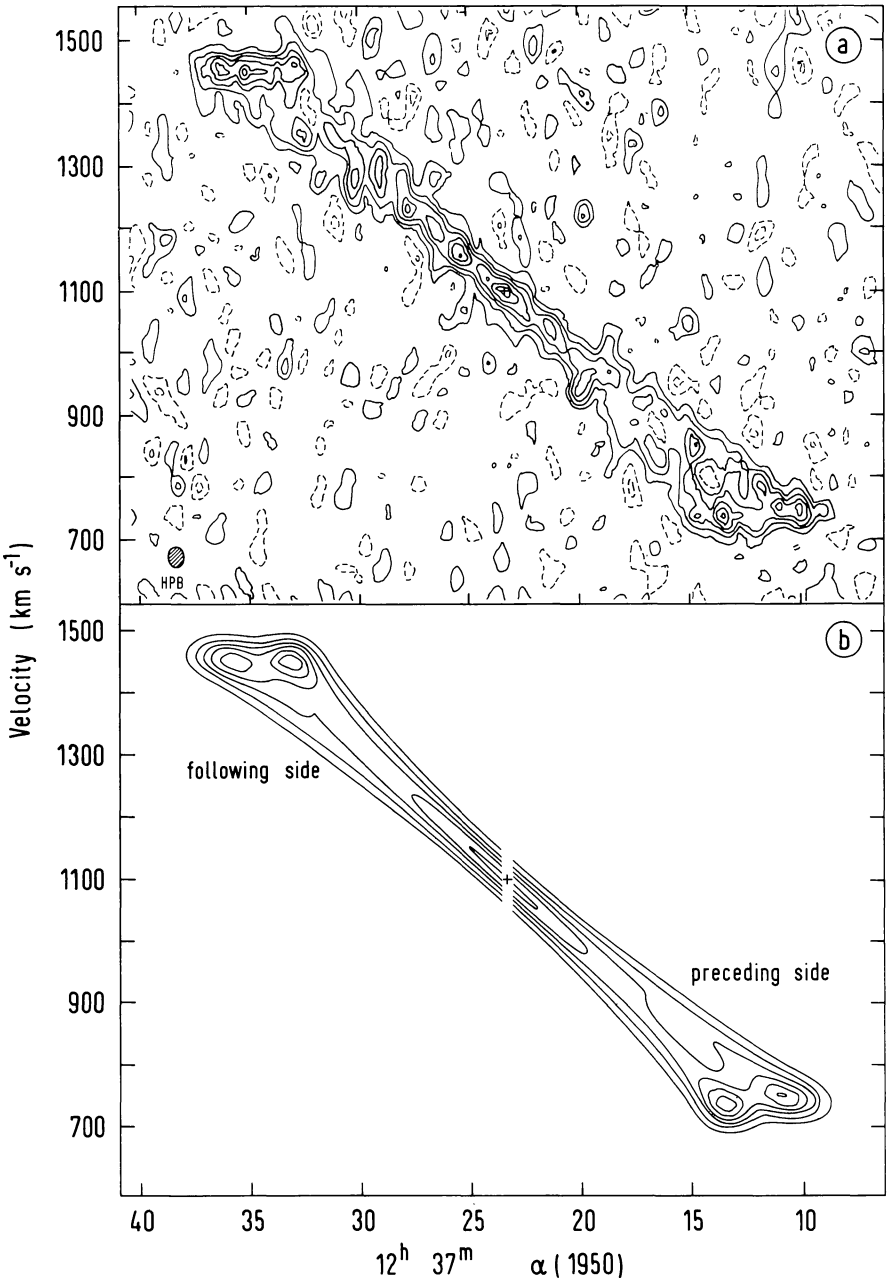

Fig. 2a and b. Map of the H I line flux from NGC 4594 plotted as a function of right ascension and velocity at the declination of the center of the galaxy. The position of the central continuum source has been marked with a cross at a velocity of 1100 km s^{-1}. **a** The observed l-v diagram; the lowest positive contour and the contour interval are 0.10 mJy arcsec^{-1}; the zero-level contour is not shown. Broken contours enclose regions whose flux level is lower than that of the surroundings (including regions of negative flux). **b** The calculated l-v diagram. Parameters used to calculate the model for the preceding and following sides of the galaxy can be found in Table 3. The model calculation is described in Section 4

3. Global results

Examination of Fig. 2a shows that the gas distribution is quite symmetric and that there is a linear run of velocity with position along the major axis. This could indicate a disk of H I rotating as a solid body or a ring of H I in circular rotation. The optical rotation curve data (see Fig. 3) and the observed distribution of gas along the major axis (Fig. 4) are inconsistent with the first possibility. Figure 3 shows the stellar rotation curves of FBGK and Schweizer (1978, which included H II velocities) superimposed on the H I l-v map, which has been symmetrized by rotating it about its position and velocity center and averaging. It is evident that the upper envelope of the H I distribution falls well below the optically determined rotation velocity out to about 120″ from the center, indicating the absence of H I from this part of the galaxy. The behaviour of the upper envelope between 120″ and 210″ suggests an approximately constant rotation velocity of about 370 km s^{-1} in this region. More accurate results can be derived from model fitting, as discussed in the following section. It appears that the optical rotation velocities, at least at all radii where H I is present, are contaminated by light from the slowly rotating bulge.

Figure 2a shows that the H I line at the projected center of the galaxy is narrow, with a full width at half power of 48 km s^{-1}. Subtracting quadratically the instrumental bandwidth (33 km s^{-1}) and the spread due to the velocity gradient across the 11″.4 beam (25 km s^{-1}) we derive an intrinsic line width of 25 km s^{-1}. This could be accounted for by the turbulent motions in the gas together with larger-scale effects like velocity gradients associated with density waves (postulating that NGC 4594 is in fact a spiral galaxy). Even without these effects it sets an upper limit to systematic radial motions in the gas of about 15 km s^{-1}, arguing against a recent origin of the gas either by accretion or by ejection from the nucleus. The peak at the projected center of the galaxy can be explained to a large extent by velocity crowding.

The regions of depressed flux level (regions surrounded by dashed contours) which show up within the maxima near both ends of the l-v diagram suggest that the H I forms two separate

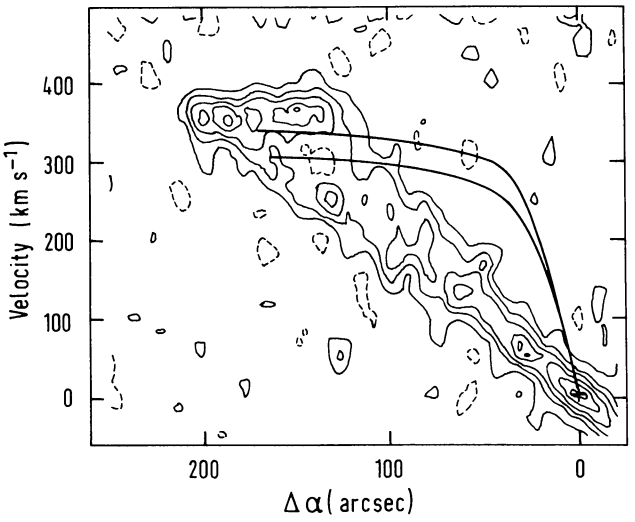

Fig. 3. Symmetrized H I distribution of NGC 4594 as a function of velocity and projected distance from the center (see text) with contours as in Fig. 2. The solid curves are the stellar rotation curve from FBGK (lower curve) and the emission line/stellar curve of Schweizer (1978) (upper curve)

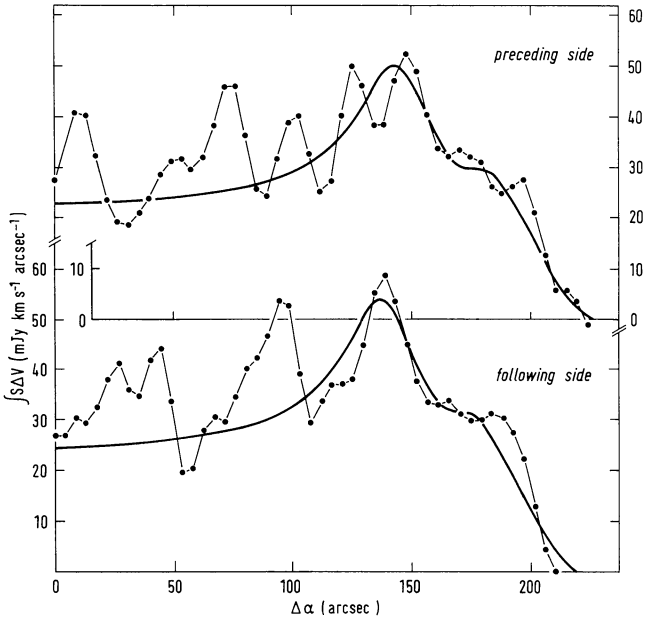

Fig. 4. Plot of the integrated H I flux along the long axis of NGC 4594. The observations are represented by connected dots, the model by a solid curve

linear structures in the l-v plane, indicating the presence of two approximately concentric rings.

The projected H I column density distribution along the major axis has been obtained by integrating the masked l-v map over all velocities. The result is shown in Fig. 4. The position of the central continuum source has been taken as the point of symmetry and the data are smoothed in right ascension with a three-point running mean. The H I distribution shown in Fig. 4 is also consistent with the assumption that the gas is distributed in two concentric rings, where the maximum at $\Delta\alpha = 140''$ can be attributed to the inner ring and the broad shoulder at $\Delta\alpha = 180''$ to the outer. The peaks inward of $\Delta\alpha = 120''$ cannot be explained in the same way because of their lower projected velocities and must be due to individual H I concentrations in the rings, with typical H I masses of 2 10^7 $M_\odot$. Their amplitudes are considerably in excess of the expected instrumental noise level of about 5 mJy km s^{-1} arcsec^{-1}. Similar concentrations in the region $\Delta\alpha >$ 120″, where the rings are seen tangentially, may influence the shapes of the terminal peaks and shoulders but will be crowded too closely to be seen individually. In these regions the behaviour of the H I column density is therefore orderly and quite similar on both sides. We note, however, that the curves are systematically displaced with respect to one another in the sense that the H I extends further on the preceding than on the following side. With the aid of the model described in Sect. 4, we find that, at least for the regions in which such a determination is possible, the center of the H I distribution lies about 300 pc westward of the coincident optical and radio continuum nuclei. This asymmetry is smaller than that which we are accustomed to find in spiral galaxies.

The global H I line profile has been obtained by integrating the l-v map over all positions after masking as above and is shown in Fig. 5; it has the characteristic two-horned shape which arises from gas in an annulus or a disk with a flat rotation curve. The line profile agrees well with that measured with the NRAO 43-meter telescope (FBGK); likewise, the two measurements of

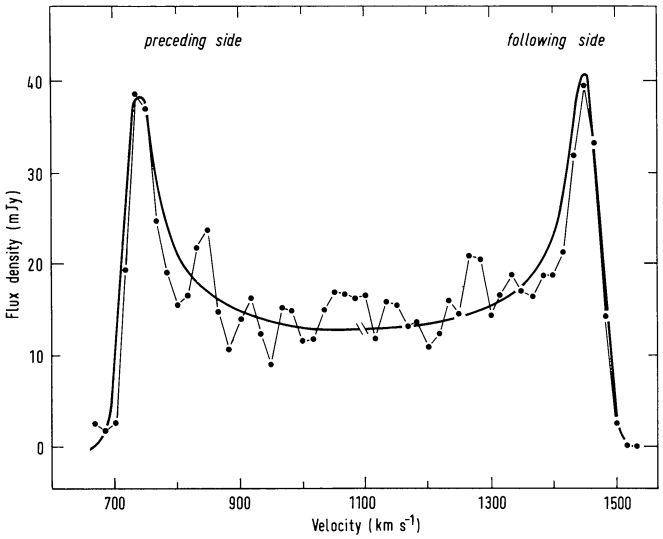

Fig. 5. Global H I line profile for NGC 4594. Observations are represented by connected dots, the model by the solid curve

the total flux in the line are in satisfactory agreement. From the WSRT profile we find $\int S\,dv = 14.2$ Jy km s^{-1}, while the value found by FBGK is 11.1 Jy km s^{-1}. Since the two types of observation lose sensitivity for quite different types of extended structures, this agreement suggests that the WSRT observations have detected essentially all of the line flux and that little if any H I has been deleted by the sidelobe correction and masking procedures or is concealed in structures larger than a few minutes of arc.

The apparent mass of H I in the galaxy is $M_{\rm H\,I} = 1.5\ 10^9\ M_\odot$ at the assumed distance of 18.6 Mpc. Saturation effects in various forms will cause this to be an underestimate. In edge-on galaxies shadowing by superposition of clouds (as opposed to H I self-absorption within clouds, which is independent of inclination) is of particular importance. We will derive in the next section a shadowing correction of 12%, leading to a corrected mass estimate $M_{\rm H\,I} = 1.3\ 10^9\ M_\odot$, and an H I to blue luminosity ratio of $[M_{\rm H\,I}/L_B] = 0.010$ (cf. FBGK). This is much smaller than the mean value for $[M_{\rm H\,I}/L_B]$ of 0.05–0.15 for Sa galaxies (Bottinelli et al., 1980) and smaller than the mean value of 0.04 for H I-rich ellipticals (Knapp, 1983). It is also close to the low end of the range of upper limits for ellipticals with no detected H I (0.003–0.05, Knapp et al., 1979).

The peaks in the line profile (Fig. 5) are at 735 and 1449 km s^{-1}, giving an approximate systemic radial velocity of 1092 km s^{-1}. A better estimate of the systemic velocity was made as follows: The l–v map was rotated through 180° about a point whose right ascension is that of the central continuum source; the velocity coordinate of the rotation center was varied until the difference between the rotated and non-rotated maps showed no systematic variation with velocity. In this way an accurate determination of the systemic radial velocity, 1100 ± 3 km s^{-1}, was made. This value has been used throughout the remainder of this paper. It agrees well with the mean velocity of the peaks of the smoothed global profile (1100 km s^{-1}), with the flux weighted mean velocity (1102 km s^{-1}) and with the value found by FBGK. However, it is slightly higher than the optically measured value given by Schweizer (1978). In deriving the systemic velocity of 1100 km s^{-1}, it has been assumed that the continuum point source coincides with the dynamical center of the galaxy. However, as has been pointed out, the slight asymmetry of the H I distribution (Fig. 4) suggests a slightly different center. Adopting this center results in a systemic velocity of 1093 km s^{-1}. Various rules of thumb may be used for estimating the rotation velocity, assuming a flat rotation curve. Identifying the rotation velocity with the peaks in Fig. 5 leads to a value of 360 km s^{-1}; using the half-maximum points on the outer flanks gives 380 km s^{-1}. The best value may be expected to lie in this range.

The global properties assumed or derived from these observations are summarized in Table 2.

Table 2. Global properties of NGC 4594

Position (1950) (Gallouët et al., 1975)
$\alpha = 12^{\rm h}37^{\rm m}22\overset{\rm s}{.}8$, $\delta = -11°21'00''$
Distance, D = 18.6 Mpc (assuming $H_0 = 55$ km s^{-1} Mpc^{-1})
Inclination, $i = 85°$ (van Houten, 1961)
Systemic velocity, $V = 1100 \pm 3$ km s^{-1} (heliocentric)
Maximum rotation velocity, $V_c(\max) = 370 \pm 10$ km s^{-1}
21-cm line flux, $\int S\,dv = 14.2$ Jy km s^{-1}
Hydrogen mass, $M_{\rm H} = 1.15\ 10^9\ M_\odot$ (observed)[a]
Blue luminosity, $L_B = 1.12\ 10^{11}\ L_{B,\odot}$(FBGK)

[a] This value is calculated directly from the total flux. Including shadowing corrections (section 4) the best estimate is $M_{\rm H\,I} = 1.3\ 10^9\ M_\odot$

4. Model calculations

The large scale distribution and kinematics of the neutral hydrogen in NGC 4594 may be described with the aid of a simple model. In constructing the model an effort has been made to include the minimum number of free parameters required to produce the main features of the l–v diagram. The adopted model has the following properties:

1. The H I is confined to a flat disk whose inclination and orientation are determined from optical observations (see Sect. 2) and is assumed to be optically thin.

2. Within this disk the H I is assumed to be distributed uniformly in azimuth, so that it can be represented as a series of concentric rings. Detailed departures from uniformity, such as clumpiness in the H I distribution or the possibility that the rings in fact approximate sections of spiral arms, have not been included. The position of the radio continuum source, which coincides closely with the optical center (de Bruyn et al., 1976), was chosen as the center of symmetry. Since the H I is not quite symmetrically distributed with respect to this position, slightly different parameters were derived for the preceding and the following halves of the galaxy.

3. Each H I ring was described by a radius R, a central surface density σ at radius R, and a radial extent W between half-density points. Various forms of the radial density distribution were allowed, but in practically all models a Gaussian form was used. The maximum number of rings used in any model was two.

4. All H I was assumed to describe circular orbits. The circular velocity Θ was assumed to be a constant within each ring.

5. A constant isotropic velocity dispersion was introduced as a free parameter. After the line profiles had been calculated, they were further convolved with the instrumental profile. The

model calculations yielded only an upper limit to the intrinsic velocity dispersion.

The model l–v diagrams were produced by integrating along lines in the plane of the galaxy and perpendicular to the line of nodes. Attenuation by the declination profile of the synthesized beam was included. The integration was carried out by summing the contributions from consecutive 50 pc intervals in the plane of the galaxy, including only those where the density was above 10% of the maximum. The 50 pc interval is sufficiently small that velocity and density gradients can be neglected. The lines of sight were spaced at 4.″5 intervals, as were the observational grid-points. The resulting map was smoothed in right ascension by the central maximum of the synthesized beam.

The choice of parameter values was determined by matching the calculated and observed l–v diagrams, where subjective criteria were used to decide upon a suitable fit. In addition to the l–v diagrams it was useful to compare the observed and calculated global line profiles (Fig. 5) and the integrated right ascension distributions (Fig. 4).

The requirement that the H I be distributed in (at least) two rings is evident from the right-ascension distribution shown in Fig. 4. The pronounced shoulder, which is practically identical on both sides, can be reproduced in no other way. The broad flat top, with one or two depressions, seen at both ends of the l–v diagram, indicates the same; a single-ring model always leads to a distribution which is sharply peaked in those directions where the ring is seen tangentially. The integrated right-ascension distribution can be used to determine all positional parameters unambiguously. When appropriate rotational velocities and velocity dispersions are introduced, minor adjustments in the other parameters are made, and account is taken of the observed asymmetry, an adequate fit with the observed l–v diagram is obtained, as shown in Fig. 2b.

This global model does not reproduce the observed clumpiness of the H I distribution in the rings. In the tangential region, $\Delta\alpha > 120''$, the clumps tend to overlap and average out, so that here the large-scale H I distribution is most clearly revealed. For this reason, and because the l–v diagram is here most sensitive to the choice of the model parameters (except for the velocity dispersion), the parameters were adjusted so as to give a good fit to the observations in this region (see Figs. 2 and 4).

It is evident from Fig. 4 that the model which fits the observations at $\Delta\alpha > 120''$ predicts too little flux at $\Delta\alpha < 120''$. The most plausible explanation for this discrepancy is cloud-cloud shadowing in the tangential region, where the highest brightness temperatures will be encountered. Since the influence of shadowing will be least in directions close to the center of the galaxy, it is here that the model flux should be fitted to the observations. This requires a 30% increase in the model H I surface density. The total flux predicted by the model then increases to 15.9 Jy km s^{-1}, which is 12% more than the observed value reported in Table 2.

We note in Fig. 4 that the model does not reproduce the steepness of the outer flanks of the shoulders. Replacing the Gaussian distribution with a rectangular one improves the fit only marginally, and introducing a more extreme assumption seems unduly artificial. A more plausible explanation is that the sharpness is due to the clumpiness of the H I in the tangential region. In view of this possibility, no further effort has been made to model the steepness of the flank with greater accuracy.

Figures 2a and 4 indicate a remarkable degree of symmetry between the preceding and following sides of the galaxy, except for the apparent displacement of about 3″ in the preceding direction with respect to the adopted center. In calculating the models, both sides were initially represented by the same parameters. Finally, the radii were adjusted to introduce the observed asymmetry. The surface densities were scaled accordingly so as to retain equally high peaks on both sides in the model l–v plot. The resulting differences in surface density are not significant relative to other sources of uncertainty.

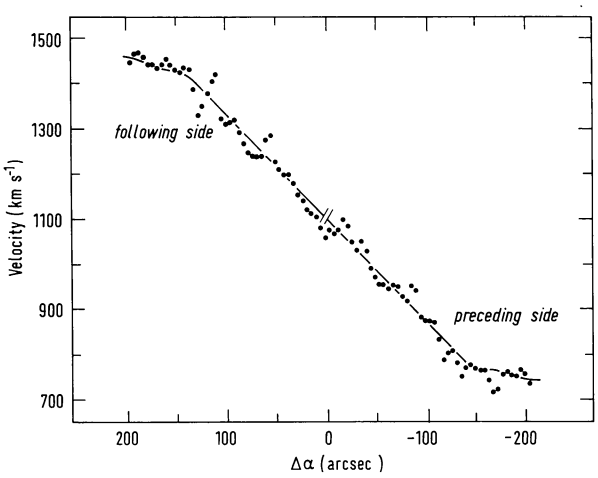

Fig. 6. The flux-weighted mean velocity as a function of distance along the long axis to the center of NGC 4594. The dots represent the observations; the solid curve is derived from the model

The rotational velocities were determined by matching the high velocity peaks in the l–v diagram on both sides of the center and by reproducing the run of flux-weighted mean velocity with right ascension (Fig. 6). On the following side, both rings show practically the same velocity; on the preceding side, the innermost ring shows a higher velocity than the outermost.

The parameters of the final model (before the 30% increase due to shadowing) are summarized in Table 3 and were used to produce the calculated curves in Figs. 2b, 4, 5 and 6. The radial extent of the H I (12–19 kpc, see Fig. 7) agrees well with the distribution of dust found by van Houten (1961). If we assume the thickness of the disk to be 100 pc then the inferred average H I space density, after correction for shadowing, is 0.8 cm^{-3}.

From the model velocities of the rings (Fig. 7), we conclude that the rotation velocity of the gas (370 km s^{-1} at $R = 15$ kpc) is constant or slightly decreasing with radius over the region where the H I is present. Examination of Fig. 3 suggests that, at all radii, the optically-measured absorption-line rotation curves are strongly affected by contamination by light from the more

Table 3. Model parameters

	Preceding side		Following side	
	Inner ring	Outer ring	Inner ring	Outer ring
R (kpc)	13.6	17.3	13.0	16.7
W (kpc)	2.3	3.2	2.3	3.2
σ_H ($M_\odot$ pc^{-2})	2.23	1.48	2.40	1.60
Θ (km s^{-1})	380	367	365	365
$\langle v^2\rangle^{1/2}$ (km s^{-1})	33	33	33	33

σ_H is the value used in calculating the model fits. The true value will be about 30% larger as a consequence of shadowing

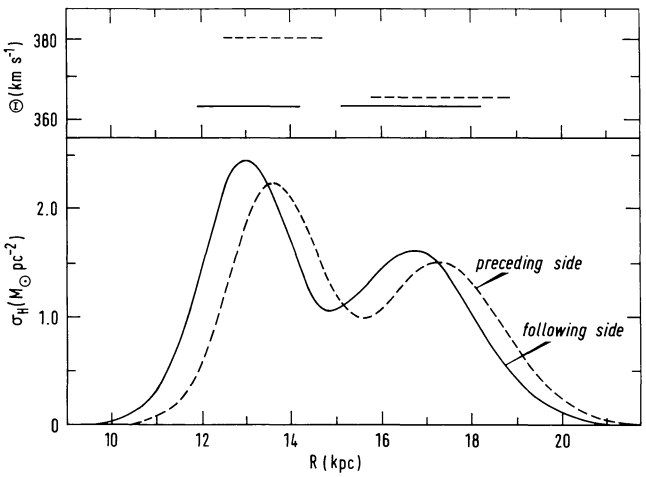

Fig. 7. Lower panel: plot of the radial H I surface density derived from the model parameters in Table 3, using a Gaussian density profile in each ring. The parameters have not been corrected for shadowing (see text). Upper panel: rotational velocities of the individual rings

slowly rotating bulge. This is indicated by the flatness of the H I rotation curve compared to the slow rise seen in the optical rotation curves, and by the differences in shape between the curve of NGC 4594 and those seen for many other galaxies (e.g. the compilations by Bosma, 1978 and Rubin et al., 1980a, b). For most galaxies, especially those of early type, the solid-body rise of the rotation curve occurs over a much shorter radial distance than it appears to do in NGC 4594, and the velocity is thereafter roughly constant. Preliminary results from new observations on which only emission lines have been measured have been communicated to us by V. Rubin (private communication). These are consistent with a rotation curve which rises rapidly to an extended flat maximum, in agreement with observations of other early-type galaxies and with the H I observations reported here.

Van Houten's (1961) deconvolution of the surface photometry of NGC 4594 suggests the presence of an exponential disk of stars which begins at a radius of about 30″, at the same location as the bend in the optical rotation curves shown in Fig. 3. This and the gradual rise of the optical curves toward the H I terminal velocity suggest that the disk spectrum is always contaminated by bulge light, with the contamination becoming less important with increasing radius. The rotation curve by Schweizer (1978) is made using both absorption and emission lines. Despite the fact that this rotation curve lies significantly below the H I velocities, Schweizer finds no systematic difference between absorption and emission velocities. The kinematics of the H II regions evidently require further study.

5. Discussion

5.1. The mass and mass-to-light ratio of NGC 4594

This subject was discussed extensively by FBGK, and the present observations add little to that discussion except to better define the range of radii over which the circular velocity is measured. The H I observations described in the preceding sections give the circular velocity, V_c, at $R = 215''$ (19 kpc) as 370 km s^{-1}, so that the mass within this radius (assuming a spherical distribution) is

$$M(R) = V_c^2 R/G \tag{1}$$

or 6 10^{11} $M_\odot$, corresponding to $[M/L_B] = 5.3$. This value provides a measurement of M/L at roughly the Holmberg radius for an elliptical-like stellar population which is in reasonable agreement with the average central values in elliptical galaxies (Faber and Gallagher, 1979).

The one-dimensional velocity dispersion, σ_*, of the bulge is 210 km s^{-1} and is roughly constant with radius, except very near the center of the galaxy (Kormendy and Illingworth, 1982). The bulge light falls with radius roughly as r^{-3} (van Houten, 1961; Burkhead, 1979). The equation of motion of the bulge stars is

$$\frac{d}{dr}[\rho_*(r)\sigma_*^2(r)] = \frac{-GM(r)\rho_*(r)}{r^2} \tag{2}$$

If we assume the mass-to-light ratio of the bulge stars to be constant, so that $\rho_*(r) \propto r^{-3}$, then Eqs. (1) and (2) give $V_c = \sigma_* \sqrt{3}$. With $V_c = 370$ km s^{-1}, we observe $V_c/\sigma_* = 1.76$, in good agreement with the above prediction. This value of V_c/σ_* and the approximate constancy of V_c within the H I annulus show that the mass in this galaxy, as in all other large galaxies observed to date, increases roughly linearly with radius in the outer regions.

5.2. The interstellar medium in NGC 4594

The observations described above show that the H I is confined to an annulus with inner and outer radii of about 130″ and 210″ within which the H I distribution is fairly smooth over a large scale. The mean surface density of the annulus projected on the plane is then 1.8 ± 0.4 10^{20} cm^{-2}. The half-density limits in radius of the dust distribution (van Houten, 1961) agree rather well with the measured extent of the H I. The mean value of the visual extinction perpendicular to the plane, A_V, in the annulus is $0^m.17$ (this may be a lower limit because of the high inclination of the galaxy), giving $N(\text{H I})/A_V \leqq 10^{21}$ atom cm^{-2} mag^{-1}, which is about half of the value in the local solar neighbourhood for the ratio of total H (H I + H_2) column density to visual extinction. Schweizer (1978) finds that there are at least two H II regions in the H I annulus of luminosity comparable to the luminosities of the brighter H II regions in the Galaxy. Thus, on the average, the interstellar matter in NGC 4594 resembles that in a spiral galaxy in its overall physical properties, as opposed to that in an elliptical or SO galaxy.

Searches for CO emission from NGC 4594 have so far yielded only upper limits, $T_A^* \lesssim 0.03$ K using the NRAO 11 m antenna, whose half power beam width is 65″ (Balick and Gallagher, unpublished). Suppose that the mass of molecular gas in the galaxy equals the mass of atomic gas and that the molecular gas has a similar radial distribution. If we assume that all of the molecular gas is in clouds like those seen in the solar neighbourhood ($T = 8$ K, $\Delta V = 5$ km s^{-1}, $r = 5$ pc, $M = 2000$ $M_\odot$) then the expected value of T_A^* (CO) is about 0.01 K, as long as the telescope used to make the observations has a beamwidth less than the radius of the galactic disk.

The observations described herein show that the H I distribution in NGC 4594 is confined to an annulus whose radial distribution is about the same as that of the dust. The symmetrized map of the distribution (Fig. 3) shows that the H I intensity integrated over ± 15 km s^{-1} at $V = 355$ km s^{-1} is at least ten times smaller at a radius of $<100''$ than in the H I annulus. While other

early-type spirals frequently show a ring-type distribution, H I emission is still detectable at 20% of the peak value almost to the center of the galaxy (e.g. the Sa galaxy NGC 7814, van der Kruit and Searle, 1982; NGC 891, Sancisi and Allen, 1979). At the present time, molecular observations have not been made to great enough sensitivity to show whether or not the hole in the H I distribution in NGC 4594 is due to molecule formation, but this is somewhat unlikely because of the close correspondence between the dust, H I and H II radial distributions.

When similar holes exist in the H I distributions in other spirals (Bosma, 1978), they roughly correspond in radius to the radius of the bulge. In our own galaxy and in M 31 (the only cases for which sufficient information exists at present) this hole is also present in molecular gas (Gordon and Burton, 1976; Stark, 1984). Several mechanisms have been considered for clearing spiral bulges of gas, including the presence of a hot, outflowing wind (Faber and Gallagher, 1976). Here we consider another mechanism, suggested by Gunn (1979), namely the loss of angular momentum of the disk gas due to collisions with gas shed by dying stars in the bulge. Assuming the latter to have zero net angular momentum, the net flux of mass inwards, for a galaxy with a flat rotation curve, is

$$\dot{M} = 2\pi r^2 \dot{\mu}$$

where $\dot{\mu}$ is the mass flux onto the disk.

Suppose that the original gas disk in NGC 4594 followed the distribution of the stellar disk. Then, if the gas in the annulus is assumed to be unperturbed at the present epoch, the original gas surface density of the disk will have been

$$\Sigma(r) = 6\ 10^{21} \exp(-0.2(r-3.3))\ \mathrm{cm}^{-2},$$

where r is in kpc. If the stellar density in the bulge decreases as r^{-3}, the total blue luminosity of the bulge is $1.2\ 10^{11}\ L_\odot$, and the rate of mass loss from dying bulge stars is $1.5\ 10^{-11}\ M_\odot\ \mathrm{yr}^{-1}\ L_\odot^{-1}$ (Faber and Gallagher, 1976), then the time scale for removal of the gas is

$$T(r) = 1.7\ 10^9 (r/3.3)^3 \exp(-0.2(r-3.3))\ \mathrm{yr}.$$

The dependence of T on r is shown in Fig. 8, where it can be seen that the radii over which the gas has sufficiently long lifetime against this effect agree with those of the gas annulus in the galaxy. Some small amount of gas continues to be transferred to the central regions of the galaxy, where it could be responsible for the continued fuelling of the central radio continuum point source.

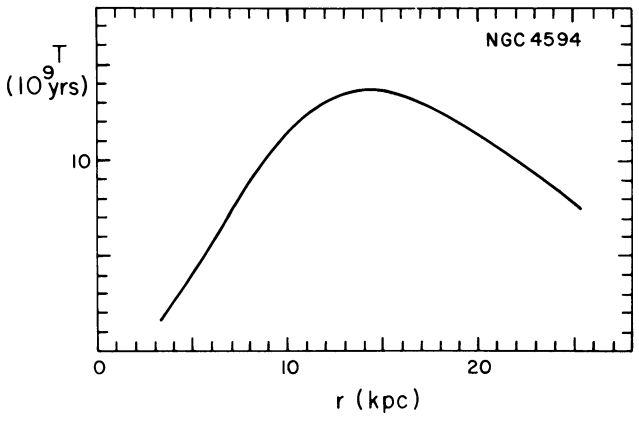

Fig. 8. Lifetime of cold gas as a function of radius in the disk of NGC 4594 against removal by angular momentum transfer with bulge stars

6. Conclusions

From aperture synthesis observations of H I in the luminous Sa galaxy NGC 4594, we have shown that:

(1) The H I lies in an annulus between 12 and 19 kpc from the center of the galaxy, with the density at radii within 12 kpc at least a factor of ten lower than in the annulus. The radial extent of the H I is coextensive with that of the dust found by van Houten (1961).

(2) At the radii where H I is detected, the rotation curve is flat at 370 ± 10 km s^{-1}. The mass of the galaxy within 19 kpc is $6.0\ 10^{11}\ M_\odot$ and the corresponding mass-to-light ratio is $5.3\ M_\odot/L_\odot$. There is no bulk radial motion of the gas greater than about 15 km s^{-1}. Comparison of the velocity fields measured by stellar absorption lines and by H I suggests that the former are contaminated by light from the more slowly-rotating spheroid.

(3) The interstellar matter in NGC 4594 resembles in its properties that in the solar neighbourhood, while star formation, as revealed by the presence of H II regions, is confined to the H I annulus. The relative H I content, $[M_H/L_B]$, is lower by a factor of order 10 than values found for other Sa galaxies, and is lower than the fractional H I content of detected ellipticals. It is likely that this is due to gas having been removed from most of the disk by interaction with the large spheroid of the galaxy.

Acknowledgements. We are very grateful to Dr. R. Sancisi for his enthusiastic and valuable help and advice, to Drs. J.E. Gunn, U.J. Schwarz and W. van Driel for many valuable discussions, to Dr. V. Icke for suggestions based on a critical reading of the manuscript and to an anonymous referee for several useful comments. The initial data reduction was carried out using the Groningen Image Processing System (GIPSY). G.R.K. acknowledges financial support from the Netherlands Organization for the Advancement of Pure Research (ZWO) for research at the Kapteyn Laboratory of the University of Groningen and is grateful to Dr. H. van Woerden and other members of the staff for their hospitality. Support was also provided through NSF grants AST-80009252 and AST-8213292 to Princeton University. E.B. acknowledges fellowship support provided by the Consejo Nacional de Investigaciones Científicas y Técnicas of Argentina and the Netherlands Foundation for Radio Astronomy (SRZM). S.M.F. acknowledges financial support from ZWO, from the Leiden Kerkhoven-Bosscha Fund and from NSF grant AST-8211551 to the University of California. The Westerbork Synthesis Radio Telescope is operated by SRZM with the financial support of ZWO.

References

Bajaja, E., Shane, W.W.: 1981, *Bol. Asoc. Argentina Astron.*, No. 26, p. 123

Bos, A., Raimond, E., van Someren Greve, H.W.: 1981, *Astron. Astrophys.* **98**, 251

Bosma, A.: 1978, The Distribution and Kinematics of Neutral Hydrogen in Spiral Galaxies of Various Morphological Types, Dissertation, University of Groningen

Bottinelli, L., Gouguenheim, L., Paturel, G.: 1980, *Astron. Astrophys.* **88**, 32

de Bruyn, A.G.: 1978, in Structure and Properties of Nearby Galaxies, IAU Symp. No. 77, eds. E.M. Berkhuijsen and R. Wielebinski, Reidel, Dordrecht, p. 205

de Bruyn, A.G., Crane, P.C., Price, R.M., Carlson, J.B.: 1976, *Astron. Astrophys.* **46**, 243
Burkhead, M.S.: 1979, in Photometry, Kinematics and Dynamics of Galaxies, ed. D.S. Evans, University of Texas, Austin, p. 143
Faber, S.M., Gallagher, J.S.: 1976, *Astrophys. J.* **204**, 365
Faber, S.M., Gallagher, J.S.: 1979, *Ann. Rev. Astron. Astrophys.* **17**, 135
Faber, S.M., Balick, B., Gallagher, J.S., Knapp, G.R.: 1977, *Astrophys. J.* **214**, 383 (FBGK)
Gallouët, L., Heidmann, N., Dampierre, F.: 1975, *Astron. Astrophys. Suppl.* **19**, 1
Gordon, M.A., Burton, W.B.: 1976, *Astrophys. J.* **208**, 346
Gunn, J.E.: 1979, in Active Galactic Nuclei, eds. C. Hazard and S. Mitton, Cambridge University Press, p. 213
Högbom, J.A.: 1974, *Astron. Astrophys. Suppl.* **15**, 417
van Houten, C.J.: 1961, *Bull. Astron. Inst. Netherland* **16**, 1
Knapp, G.R.: 1983, in Internal Kinematics and Dynamics of Galaxies, IAU Symp. No. 100, ed. E. Athanassoula, Reidel, Dordrecht, p. 297
Knapp, G.R., Kerr, F.J., Henderson, A.P.: 1979, *Astrophys. J.* **234**, 448
Kormendy, J., Illingworth, G.: 1982, *Astrophys. J.* **256**, 460
van der Kruit, P.C., Searle, L.: 1982, *Astron. Astrophys.* **110**, 79
Rubin, V.C., Ford, W.K., Thonnard, N.: 1980a, *Astrophys. J.* **238**, 471
Rubin, V.C., Burstein, D., Thonnard, N.: 1980b, *Astrophys. J. Letters* **242**, L149
Sancisi, R., Allen, R.J.: 1979, *Astron. Astrophys.* **74**, 73
Schweizer, F.: 1978, *Astrophys. J.* **220**, 98
Shaffer, D.B., Marscher, A.P.: 1979, *Astrophys. J. Letters* **233**, L105
Stark, A.A.: 1984, IAU *Symp.* No. 106, ed. H. van Woerden (in press)
Williams, T.B.: 1977, *Astrophys. J.* **214**, 685